Engineering Structures 203 (2020) 109859

Contents lists available at ScienceDirect

Engineering Structures

journal homepage: www.elsevier.com/locate/engstruct

Measuring bridge frequencies by a test vehicle in non-moving and moving states

Y.B. Yang[a,b,c], Hao Xu[a,b,*], Bin Zhang[a,b], Feng Xiong[a,b], Z.L. Wang[a,b]

[a] School of Civil Engineering, Chongqing University, Chongqing 400045, China
[b] MOE Key Lab. of New Techno. for Construction of Cities in Mountain Area, Chongqing Univ., China
[c] Dept. of Construction Eng., National Yunlin Univ. of Science and Technology, Yunlin, Taiwan, China

ARTICLE INFO

Keywords:
Bridge
Contact point
Field test
Frequency
Torsional frequency
Vehicle scanning method

ABSTRACT

This paper presents the measurement results of bridge frequencies by a test vehicle in non-moving and moving states. The self-made test vehicle fitted with vibration sensors is a two-wheel trailer, intentionally used to simulate the theoretical single degree-of-freedom system. The two-span bridge selected is located in the Chongqing University campus. For the purpose of comparison, the bridge frequencies were firstly measured by direct deployment of vibration sensors on the bridge. The dynamic properties of the test vehicle in the non-moving state, including the transmissibility, are examined in detail. Based on the measured car-body response, the contact-point response of the vehicle with the bridge was calculated by a backward procedure that allows the vehicle frequency to be eliminated. It was found that the vehicle in the non-moving state can catch more bridge frequencies than in the moving state. Both the car-body and contact-point responses agree well the results by direct measurement. But the contact-point response performs better than the car-body response, which can be used to detect the first few frequencies of the bridge, including the torsional frequency.

1. Introduction

The strength limits of existing bridges can be estimated by the static applied load tests, but their health conditions should better be detected by the vibration-based methods. Most modern applications of the vibration data for detecting the soundness of bridges began in the 1970s [1–3]. It is believed that vibration-based structure health monitoring is necessary for structures susceptible to ageing and the associated risk of accumulated damages [4,5]. Modal parameters such as frequencies, mode shapes and damping ratios are the key characteristics that are of concern most of the time. The health condition of a bridge can be diagnosed through the variation of the modal parameters identified for the bridge. In order to obtain the vibration data of the bridge, the effects of natural phenomena, such as ambient vibrations [1,2], truck impact loads [6], earthquakes [7], traffic flows [8,9] and even typhoons [10], have been utilized as excitations for the bridge. Some reviews of the vibration-based structure health monitoring using the vibration data collected from the bridge are available in Refs. [11–13].

Conventionally, the *direct method* has been adopted in measuring the vibration of a bridge, which is featured by the installation of a large number of vibration sensors on the bridge. Such a method requires a fixed monitoring system, which is generally costly either in deployment or in maintenance. This method allows the bridge response to be constantly measured, but it also creates a huge amount of data that cannot be effectively digested. In addition, the sensors and equipment installed on a bridge can hardly be transplanted to another bridge, since they have been designed on a one-system-per-bridge basis. Partly due to the above constraints, only a limited number of bridges or certain parts thereof that are functionally important have been equipped with sensors and devices for long-term monitoring.

To overcome the drawbacks with the direct method, Yang et al. proposed the *indirect method* in 2004 for retrieving the bridge frequencies from the dynamic response of a passing vehicle [14], which was later renamed as the *vehicle scanning method* (VSM) for bridges for its better conveyance of the meaning contained [15]. Compared with the direct method, the VSM only requires one or few vibration sensors to be installed on the test vehicle. The advantage with this method is obvious: mobility, economy, and practicality. Since the advent of the method, endeavors have been undertaken to retrieve the other two modal parameters, i.e., mode shapes and damping ratios, of the bridge using various approaches [16–20].

In the original formulation of the theory for the VSM, the test vehicle was assumed to be a single degree-of-freedom (DOF) system [14]. Along these lines, various improvement techniques were proposed by

* Corresponding author at: School of Civil Engineering, Chongqing University, Chongqing 400045, China.
E-mail address: hxu@cqu.edu.cn (H. Xu).

https://doi.org/10.1016/j.engstruct.2019.109859
Received 5 June 2019; Received in revised form 20 September 2019; Accepted 25 October 2019

Yang and co-workers, including the identification of the key parameters involved in scanning [21], use of the empirical mode decomposition to enhance the visibility of higher bridge frequencies [22], use of two connected vehicles to reduce the surface roughness effect [23], and suppression of the vehicle frequency by the filtering techniques [24] or proposal of the contact-point response as a better parameter [25]. For the purpose of enhancing the stability of the test vehicle while retrieving more bridge information, a two-axle test vehicle [26], which is essentially a two-DOF system, was theoretically investigated.

The aforementioned researches were focused mainly on identification of the modal parameters for bridges. To extend the capability of the VSM to damage identification of bridges, the following techniques have been attempted by researchers: wavelet-based method [27,28], pseudo-static approach [29], mode shape-based method [30–32], genetic algorithm-based method [33], wave number-based technique [34], and use of instantaneous amplitude squared [35], among others.

In the initial stage of research on the VSM, efforts have been placed mainly on the theoretical aspect. To verify the feasibility of the VSM for bridges, the fundamental frequency of the bridge was firstly extracted in the field test [36,37]. Also, a hand-drawn cart was adopted for the bridge frequency measurement, aimed at drawing the qualitative guidelines for the design of test vehicles [38]. A scaled model [39] was tested to verify the feasibility of damage detection in the laboratory. For a more complete coverage of the related works on applications of the VSM, readers are referred to the two review papers in Refs. [40,41].

Previously, relatively few studies have been presented for the VSM with the test vehicle set both in the *non-moving* and *moving states*. This paper is aimed at filling such a gap. In the non-moving state, the number of bridge frequencies extracted by the test vehicle is *no less* than the direct method, and in the moving state, two frequencies of the bridge are extracted, as an improvement over the previous field test [36]. The contact-point response of the vehicle was firstly proved in field to be better than the vehicle response for extracting bridge frequencies. The organization of the paper is as follows. To start, the configuration of the test bridge will be described. Then, the bridge frequencies will be first measured using the sensors directly attached on the bridge surface. Due to the lack of structural data for conducting the numerical analysis, these data serve as the basis for comparison with the measurement by the test vehicle. Then the considerations for designing the two-wheel test vehicle will be described in detail. The field measurement will be conducted by setting the test vehicle set either in the non-moving or moving states. In the non-moving state, the characteristics of the test vehicle, including the transmissibility and calculated contact-point response, will be studied. In the moving state, the applicability of the test vehicle to retrieving bridge frequencies will be demonstrated, along with a discussion on the limits of the technique used. Finally, some conclusions will be made.

2. Description of the test bridge

The test bridge is called the Turtle Mountain Bridge located inside Campus B of the Chongqing University in Chongqing City, China. The bridge is a two-span concrete box girder bridge with and internal hinge support and a total length of 55.2 m, as shown in Fig. 1, of which the length of one span is 29.2 m, and the other is 26 m. Both ends of the bridge are simple supports. The width of the bridge deck is 5.2 m, and the height is 1.6 m as in Fig. 2. This bridge is the one to be used both in the vehicle scanning test and comparison test in this paper.

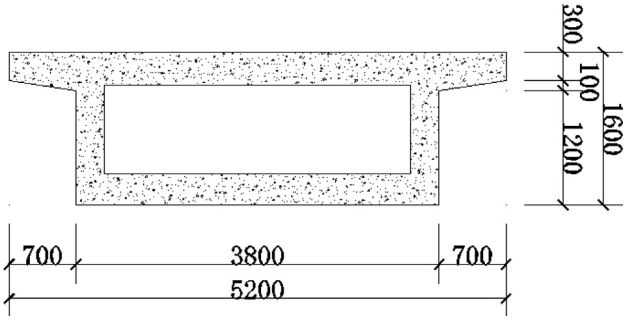

Fig. 2. Cross section of the beam (in mm).

The bridge is chosen mainly for its easiness to access by the graduate students in testing the quality of the self-made test vehicle. However, the bridge is not perfect for the following reasons: (1) Except for the exterior dimensions, no data are available for the material properties or geometry of the cross section. The internal dimensions of the cross section shown in Fig. 2 were back-calculated by calibration with the measured frequencies of the beam using estimated material properties. (2) The pavement appears to be not good due to frequent passage of heavy trucks, as shown in Fig. 3(a). (3) As an overpass for the G75 national expressway, see Fig. 3(b), the bridge suffers seriously from the vibrations and noises transmitted via the three piers by the heavy traffic underneath. (4) The bridge is too rigid to be excited, since it has a small length-to-width ratio, as will be evidenced in the field test.

For the test bridge with the single-cell cross section shown in Fig. 2, it was suspected that the torsional frequencies of vibration may be as prominent as the flexural (vertical) frequencies. This will be verified later on.

3. Measurement by sensors deployed on the bridge surface

Due to the lack of structural data for the bridge, no numerical simulation can be conducted for comparison. To offer a reference for comparison with the results by the test vehicle in the non-moving and moving states, vibration sensors were firstly installed on the bridge surface to measure the bridge frequencies, as will be presented below.

3.1. Arrangement of measurement points

With reference to Fig. 4 for the bridge deck, three rows of measuring points are arranged from the top (north) to the bottom (south) side, namely, A4-A12, B1-B16 and C4-C12. As can be seen, there is a total of 34 measurement points, with 9 points each in row A and C and 16 points in row B. The measurement points have been named such that points with the same alphabetical number, e.g., A4, B4 and C4, belong to the group of the same cross section. Except for the two measurement points in row B near each end of the bridge, the distance between any two adjacent groups is 4 m. The measurement point B9 is basically located at the position above the middle pier, with which the vibration of the pier can be detected. The sensors mounted on rows A and C enable us to measure the torsional frequencies of the bridge.

The vibrations sensors used are of the acceleration type with a model type of PCB 352C33, made by PCB Piezotronics Inc., of which the

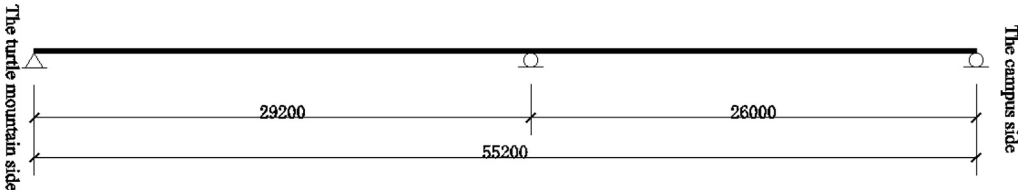

Fig. 1. Two-span test bridge (in mm).

Fig. 3. Test bridge: (a) pavement surface; (b) side view and underneath traffic.

frequency range is 0.5–10,000 Hz and the sampling rate is 1,000 Hz. Throughout all the tests, only the vertical vibration of the bridge will be measured.

3.2. Result of direct measurement

In the beginning, a large amount of vibration data was taken for the bridge under the ambient vibrations. Unfortunately, the result of these tests was unsuccessful and no frequencies of the bridge could be identified. The main reasons for this are: (1) The vibration signal of the bridge is masked by the large environmental noise transmitted from the underlying G75 national expressway. (2) The bridge is relatively stiff and hard to deform due to its relatively small length-to-width ratio.

Next, a truck weighing about 6.8 tons was employed to excite the bridge response. By letting the truck slowly pass the bridge four times, a total of 136 sets of data are recorded. Since the truck has its own excitation frequencies, such as the structural and engine frequencies, all these were carried over to the bridge. In addition, the frequencies of the test bridge also vary due to the presence of the heavy truck. Thus, the idea of using a heavy truck to excite the bridge response is considered not a good one.

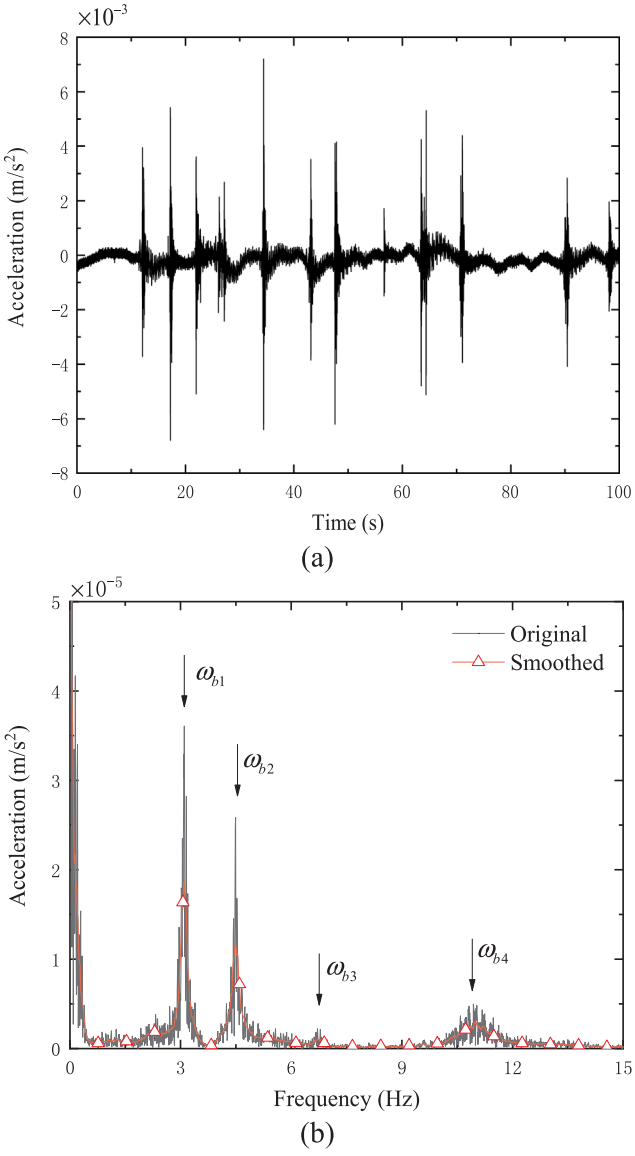

Fig. 5. Responses of measurement point B12: (a) acceleration; (b) spectrum.

To resolve the problem with the source of excitation, a group of eight students were invited to jump randomly and continuously on the bridge during the measurement. This appears to be a better way for exciting the bridge, as the weight of the students is negligible compared with that of the bridge. Under this excitation, measurements were successfully taken for the bridge, as will be presented below. The

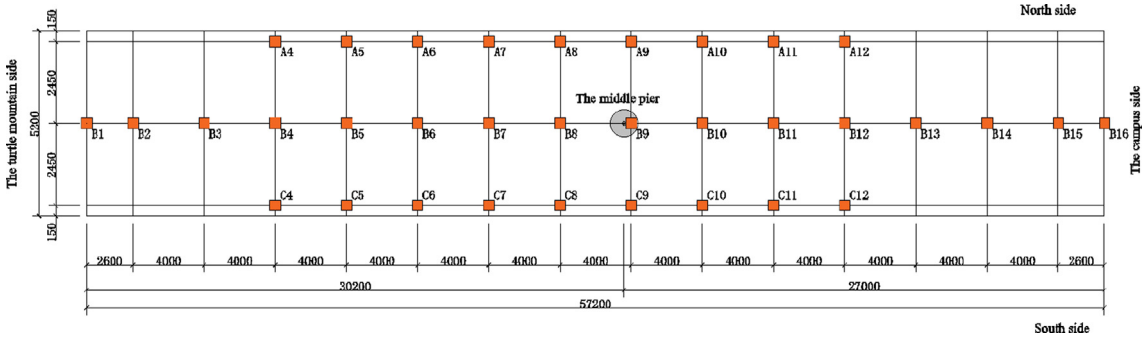

Fig. 4. Arrangement of measuring points and sensors on the bridge surface (in mm).

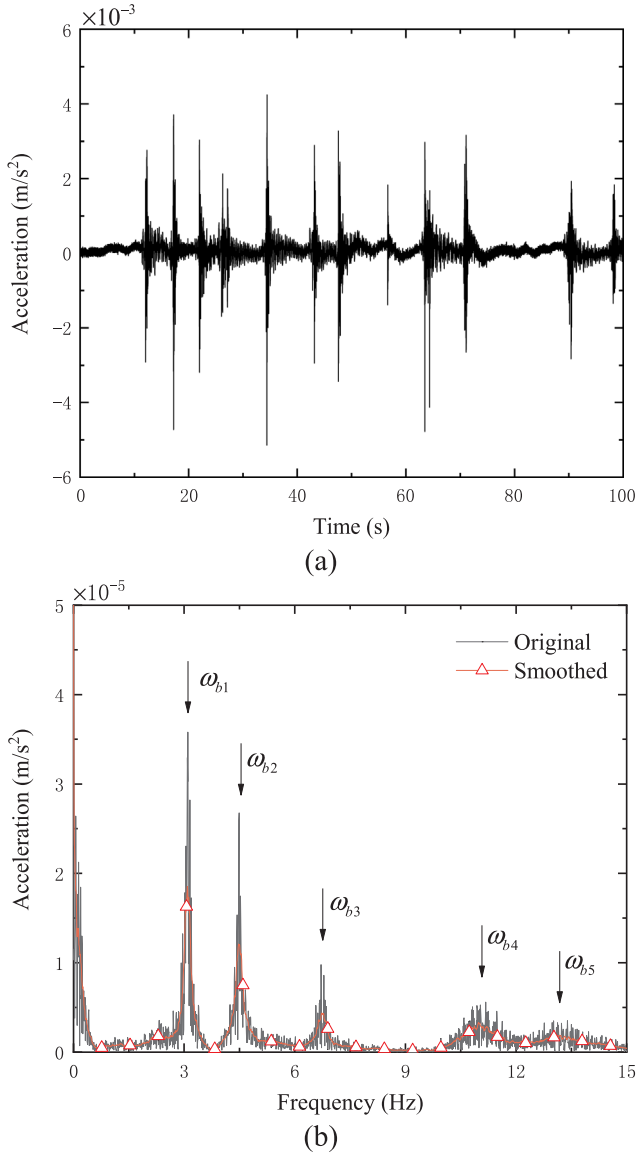

Fig. 6. Responses of measurement point C12: (a) acceleration; (b) spectrum.

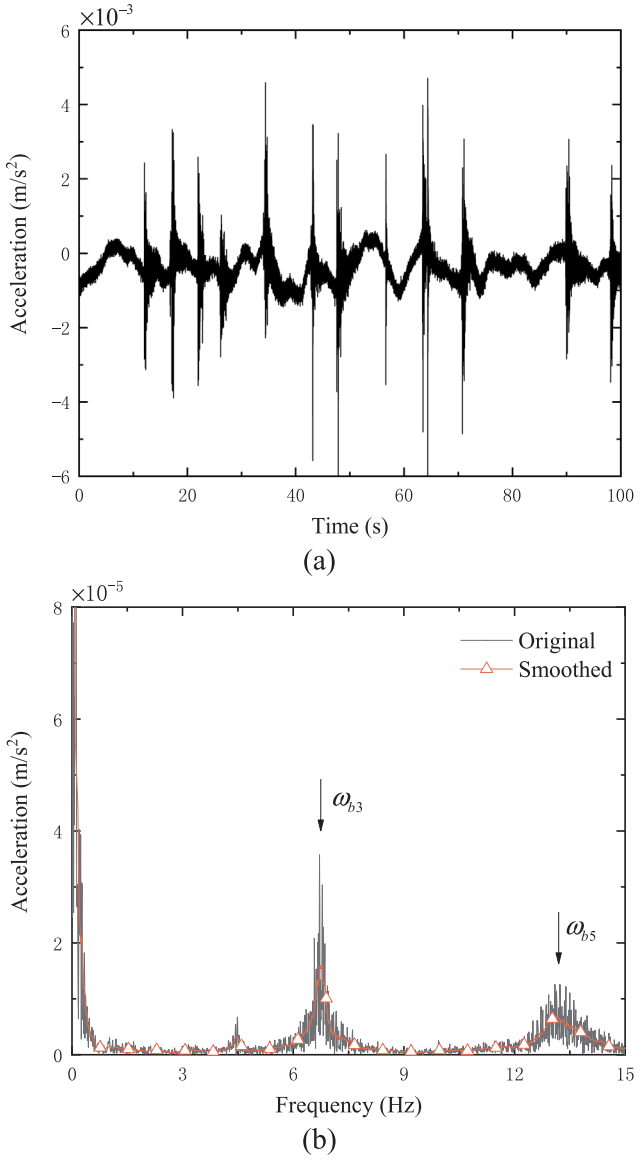

Fig. 7. Torsional responses of cross section 12: (a) acceleration; (b) spectrum.

sampling rate adopted of the sensors is 0.001 s.

The time-history acceleration response taken of point B12 on the *central line* of the bridge has been plotted in Fig. 5(a), from which the impact effect of jumping on the bridge can be clearly observed. The fast Fourier transform (FFT) of the data recorded at point B12 was presented as the black curve in Fig. 5(b). Also shown in Fig. 5(b) is the smoothed spectrum obtained via processing of the data by the moving average filter (MAF), shown as the red curve [42], which was employed to make the relevant frequencies in the spectrum more visible. From the result in Fig. 5(b), one observes that there are four distinct peaks in the acceleration spectrum, marked as ω_{b1}, ω_{b2}, ω_{b3} and ω_{b4} sequentially. Moreover, the amplitude of ω_{b3} is relatively small, and ω_{b4} is a wide peak. The zero-frequency peak is caused by the low-frequency noises from the environment.

Further effort was undertaken to clarify whether the frequencies in Fig. 5(b) are related to the flexural (vertical) or torsional motions of the bridge. To this end, measurement was conducted for points A12 and C12 on the *two sides* of the bridge. To save the paper length, only the time-history acceleration and spectra, of point C12 were plotted in Fig. 6(a) and (b), respectively. Here, the first five frequencies identified from the acceleration spectrum for the bridge in Fig. 6(b) are marked as ω_{b1}, ω_{b2}, ω_{b3}, ω_{b4} and ω_{b5} sequentially, in which the frequency ω_{b5} is also a wide peak. A comparison of Fig. 6(b) with Fig. 5(b) indicated that: (1) The measurement points on the two sides of the bridge allow us to identify more bridge frequencies, e.g., the frequency ω_{b5} is present only in the result for point C12. (2) The amplitude of ω_{b3} measured from C12 appears to be much greater than that for B12. (3) The amplitudes of the frequencies ω_{b1}, ω_{b2} and ω_{b4} in the two figures are similar.

To identify the torsional frequencies involved in the previous results, the acceleration data taken of point A12 were deducted by those of point C12 points, and then divided by the bridge width, to yield the *torsional* acceleration and spectra in Fig. 7(a) and (b), respectively. The result in Fig. 7(b) indicates clearly that both ω_{b3} and ω_{b5} are the torsional frequencies of the bridge. Consequently, it is inferred that the three frequencies ω_{b1}, ω_{b2} and ω_{b4} are related to the flexural (vertical) modes of the bridge. Both the frequencies ω_{b4} and ω_{b5} cover a wide range, likely to be caused by multi close frequencies.

The first five frequencies of the bridge identified are listed in Table 1, in which the vibration direction of each frequency has been identified. The fundamental frequency of the bridge is 3.08 Hz. It should be noted that the bridge is relatively stiff, as can be judged from the relatively small amplitudes of vibration in Figs. 5(a), 6(a) and 7(a), when subjected to the jumping of a group of people. The experience

Table 1
Bridge frequencies identified by direct measurement.

ω_b	ω_{b1} (flexural)	ω_{b2} (flexural)	ω_{b3} (torsional)	ω_{b4} (flexural)	ω_{b5} (torsional)
Frequency(Hz)	3.08	4.49	6.78	11.00	13.09

with the direct measurement above is that it is generally costly, laborious, and time-consuming for a successful test to be conducted, as there are many technical issues that need to be handled perfectly on site. In contrast, basically the same result can be achieved using a test vehicle, especially in the non-moving state, as will be demonstrated later on.

4. Design of the test vehicle

In this study, a test vehicle that forms the core of the experiment was designed and manufactured locally. The following is a brief summary of its mechanical properties.

4.1. Description of the test vehicle

The top and side views of the self-designed test vehicle are shown in Fig. 8(a) and (b), along with a picture showing the test vehicle resting on the bridge in Fig. 9. The test vehicle is actually a two-wheel trailer, with no suspension system. Since it cannot move by itself, it was towed by a 1.5 t four-wheel ordinary car (Mazda CX4) as the tractor during the field test. The test vehicle was painted with a conspicuous yellow color and affixed with reflective tapes for traffic safety. The car body is made of steel, weighing about 0.9 t, and has a total length of 2.98 m and a total width of 1.81 m. In this study, the two-wheel test cart is intentionally used to mimic the single-DOF system adopted in previous theoretical investigations [14,15,41]. Three vibration sensors, also of the PCB 352C33 type, are installed each on the left, center and right sides of the axle of the test vehicle, as shown in Fig. 8(a). The central sensor mounted above the axle is mainly used to measure vertical vibration and frequencies of the bridge, and the left and right sensors are used to detect the torsional vibration and frequencies of the bridge.

To enhance its stability or maneuverability in moving, the test cart

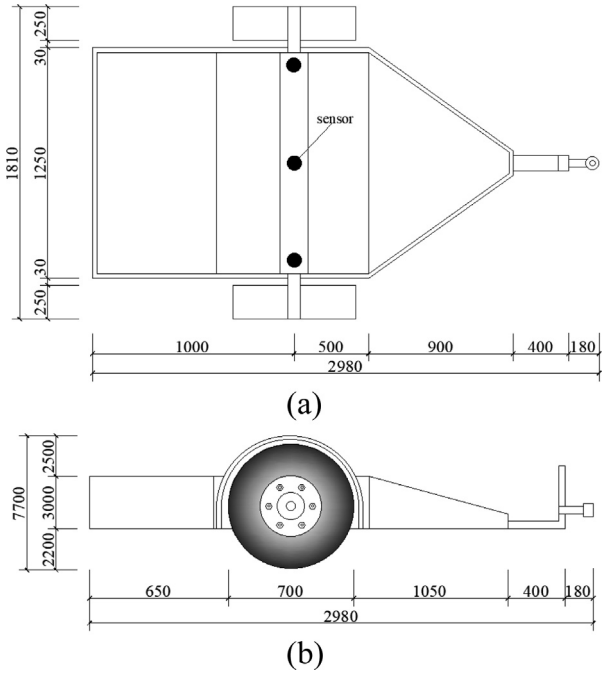

Fig. 8. Design drawings: (a) top view; (b) side view (in mm).

Fig. 9. Self-designed test vehicle resting on the bridge.

is designed such that the center of gravity is always located beneath the axle. On the two sides of the axle, i.e., near the wheels, space is reserved for mounting additional metal plates, to increase the weight of the vehicle such that better stability can be achieved at a higher moving speed [38].

According to the experiments in Ref. [38], a test vehicle with solid tires performs better on the bridge surface with roughness. So, a pair of solid rubber tires, as shown in Fig. 10, is adopted to increase the stiffness of the test vehicle, based on the consideration that the greater the stiffness of the car body, the higher the vehicle frequency ω_v. Also, it was known that for $\sqrt{2}\omega_v > \omega_{bi}$, the absolute value of the frequency response function (FRF) will be greater than unity [25], meaning that the motion of the bridge transmitted to the test vehicle will be amplified. In this case, better results can be achieved for the VSM technique.

The data collection system adopted includes the vibration sensors, special-purpose software, and data acquisition device. The software of

Fig. 10. Solid rubber tire.

Fig. 11. Linkage between the test cart and the tractor.

the data collection system is written based on the LabVIEW of National Instruments Co. (NI), and the data acquisition device adopted is NI 9234, which has a maximum sampling rate of 51.2 kHz and a dynamic acquisition range of 102 dB. In order to ensure the stable operation of the equipment, the data acquisition device is placed inside the tractor.

The connection or linkage between the test vehicle and the tractor was also shown in Fig. 11. A square column with a steel sleeve is erected in the front of the test vehicle, which can be adjusted to meet the height of the point of the tractor, while keeping the test vehicle in the horizontal position. In order to isolate the transmission of vibrations from the tractor to the test vehicle, a pair of rubber pads are inserted at the joint. It should be noted that the connection used herein is of the semi-rigid type, which is considered to be better for traffic safety.

5. Measurement by the test vehicle in the non-moving state

The key concern of the VSM technique is that the vibration of the bridge can be transmitted faithfully to the car body of the test vehicle. In this regard, the transmissibility of the test vehicle connected with the tractor with the engine set off is first investigated. Since the bridge is very stiff, the weight or location of the tractor on vibration of the bridge is considered negligible. The vibration data collected from the acceleration sensor mounted on the vehicle will be compared with those from another sensor fixed at a point near the vehicle's contact-point on the bridge surface. Under the excitation of random jumping by a group of people, responses were recorded simultaneously for both sensors on the vehicle and on the bridge.

The acceleration response of the bridge has been shown in Fig. 12(a), from which the impact effect of jumping can be identified. Correspondingly, the FFT spectra of the bridge response have been plotted in Fig. 12(b), from which five frequencies can be identified. For comparison, the acceleration response and FFT spectra of the test vehicle have been plotted in Fig. 13(a) and (b), respectively. A comparison of Fig. 12(b) with Fig. 13(b) indicates that all the bridge frequencies have been clearly transmitted to the vehicle. Besides, it was found that the vehicle frequency is present in the vehicle response of Fig. 13(b), as was expected. It was known that in cases when the vehicle frequency has a high peak, it will bring some masking effect on the bridge frequencies, making the latter hard to identify. Hopefully this is not the case encountered herein. Another observation is that the zero-frequency leakage in Fig. 12(b) is not present in the vehicle response in Fig. 13(b).

6. Contact-point response of the test vehicle

The response of the vehicle's *contact point* with the bridge has been demonstrated to be a parameter better than the vehicle response for

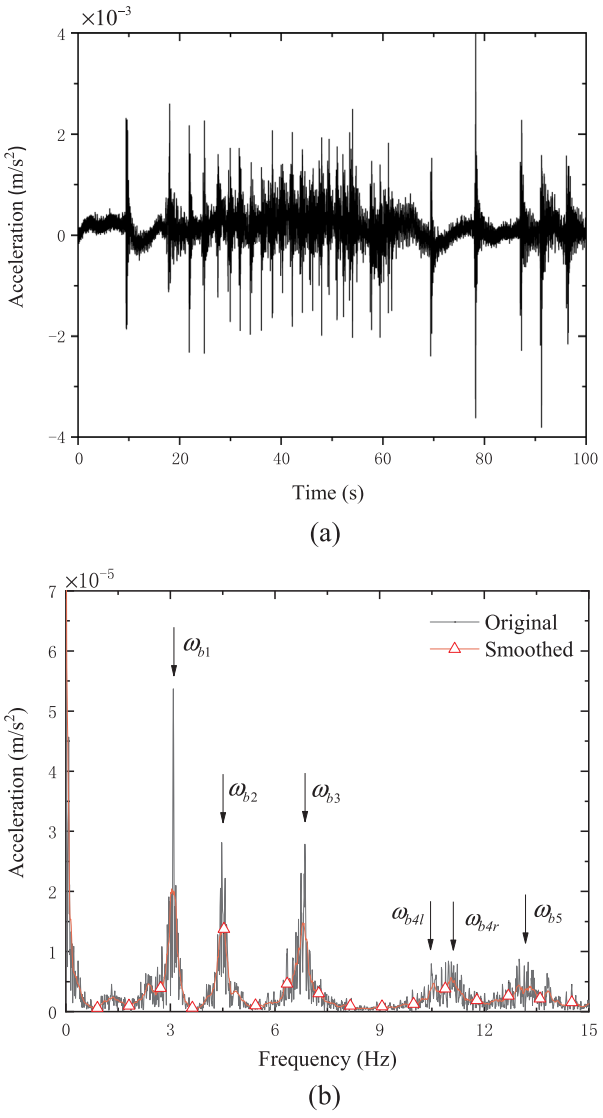

Fig. 12. Responses of bridge: (a) acceleration; (b) spectrum.

retrieving the modal properties of the bridge, since it is free of the vehicle frequency [25]. For the single-DOF test vehicle shown in Fig. 14, the equation of motion for the vehicle ignoring the damping effect is

$$m_v\ddot{y}_v + k_v(y_v - u_c) = 0, \tag{1}$$

where m_v and k_v denote the mass and stiffness, respectively, and y_v the displacement of the vehicle, and u_c the displacement of the vehicle's contact point on the bridge. Based on Eq. (1), the contact-point acceleration $\ddot{u}_c$ can be related to the vehicle acceleration $\ddot{y}_v$ as

$$\ddot{u}_c = \ddot{y}_v + \frac{d^2\ddot{y}_v}{\omega_v^2 dt^2}, \tag{2}$$

where ω_v is the vehicle frequency. Since the accelerations recorded by the vehicle are discrete data, the term $d^2\ddot{y}_v/dt^2$ can be easily replaced by the central difference as

$$\frac{d^2\ddot{y}_v}{dt^2} = \frac{\ddot{y}_v|_{i+1} - 2\ddot{y}_v|_i + \ddot{y}_v|_{i-1}}{(\Delta t)^2}, \tag{3}$$

where i denotes the ith sampling point and Δt the sampling interval. One advantage with the contact-point response $\ddot{u}_c$ calculated above is that the vehicle frequency ω_v has been eliminated. This has made the contact-point response a better parameter than the car-body response,

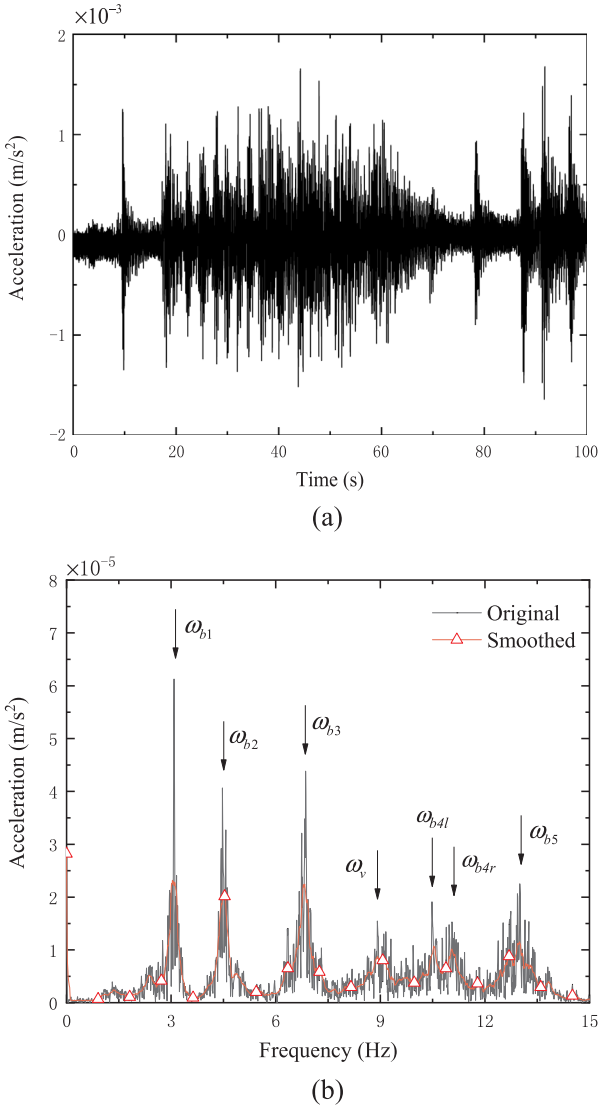

Fig. 13. Responses of test vehicle resting on bridge: (a) acceleration; (b) spectrum.

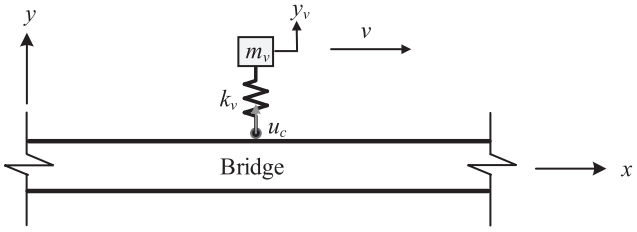

Fig. 14. Theoretical model of the test vehicle.

since the disturbing effect of the vehicle frequency has been totally removed. The above procedure remains valid for all types of bridges.

Using the above procedure, the acceleration response and FFT spectra of the vehicle's contact point have been plotted in Fig. 15(a) and (b), respectively. An observation of Fig. 15(b) is that *the vehicle frequency has been filtered out*, as expected. For comparison, the FFT spectra of the bridge, test vehicle and contact point without and with the smoothing technique have been plotted in Fig. 16(a) and (b), respectively. The following are observed: (1) The bridge frequency ω_v (=9.09 Hz) that has been disturbing in application of the VSM technique exists only in the vehicle response, but not in the contact-point or

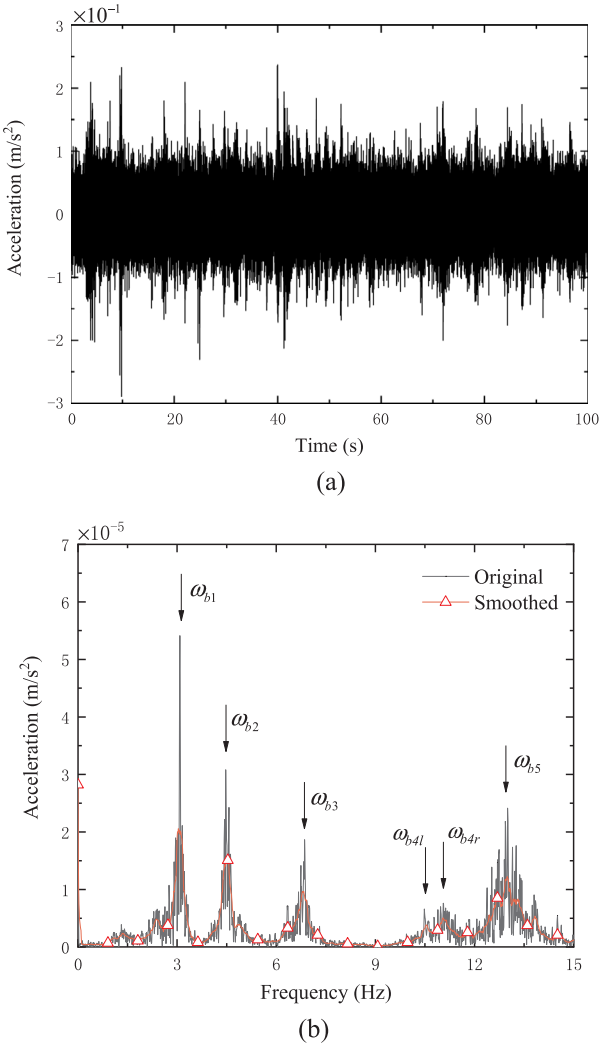

Fig. 15. Contact-point responses of test vehicle resting on bridge: (a) acceleration; (b) spectrum.

bridge responses. (2) Five identical frequencies of the bridge can be identified from the bridge, vehicle and contact-point responses, same as those by direct measurement. (3) The contact-point response is free of the vehicle frequency ω_v, an advantage pointed out in Ref. [25], which also compares well with the bridge response, as judged by the shape of the spectra and the number of peaks. (4) The shifted frequencies ω_{b4l} and ω_{b4r} are more distinct in the vehicle response. (5) The amplitudes in the vehicle response are greater than those of the bridge and contact-point responses for the first four bridge frequencies due to the satisfaction of the condition $\sqrt{2}\omega_v > \omega_{bi}$ with $i = 4$, as indicated by the dashed line [25]. (6) The fifth bridge frequency ω_{b5} is more evident in the contact-point response than the other two responses.

Based on the above analysis, the transmissibility of the test vehicle in the non-moving state is confirmed to be good, in that the test vehicle can faithfully reflect the first few frequencies of the bridge, including both the flexural and torsional frequencies. Moreover, the contact-point response outperforms the vehicle response in that more bridge frequencies can be identified, while the disturbing effect of the vehicle frequency has been eliminated.

7. Measurement by the test vehicle in the moving state

In the previous sections, the bridge frequencies were firstly measured by sensors directly mounted on the bridge, which serve as the reference for comparison. Then the transmissibility of the test vehicle in

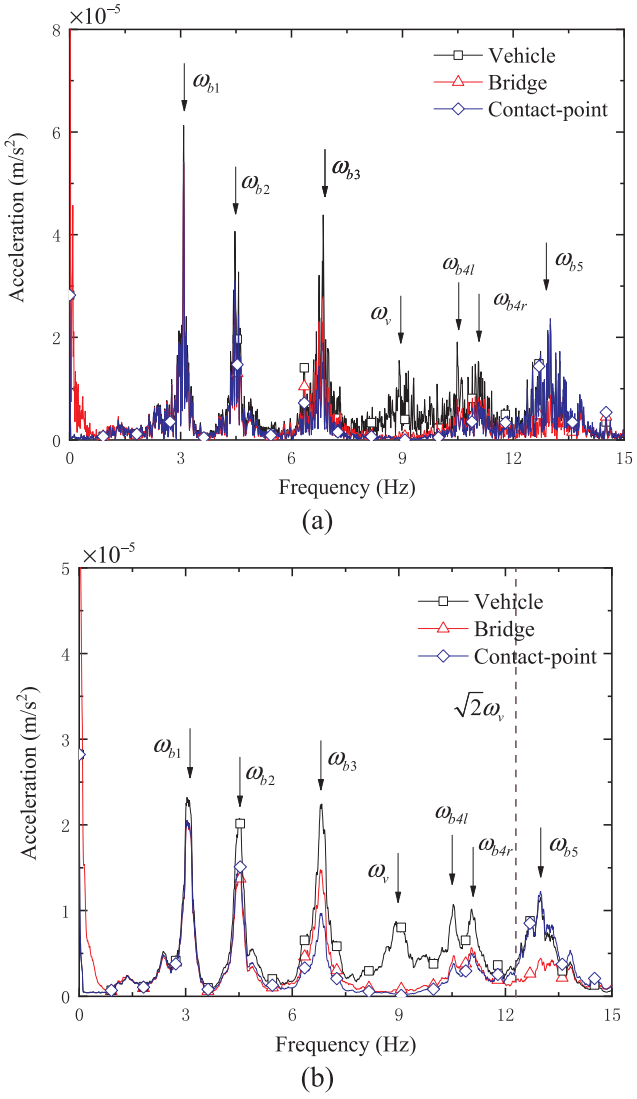

Fig. 16. Comparison of bridge frequencies extracted from vehicle, bridge and contact point: (a) original; (b) smoothed.

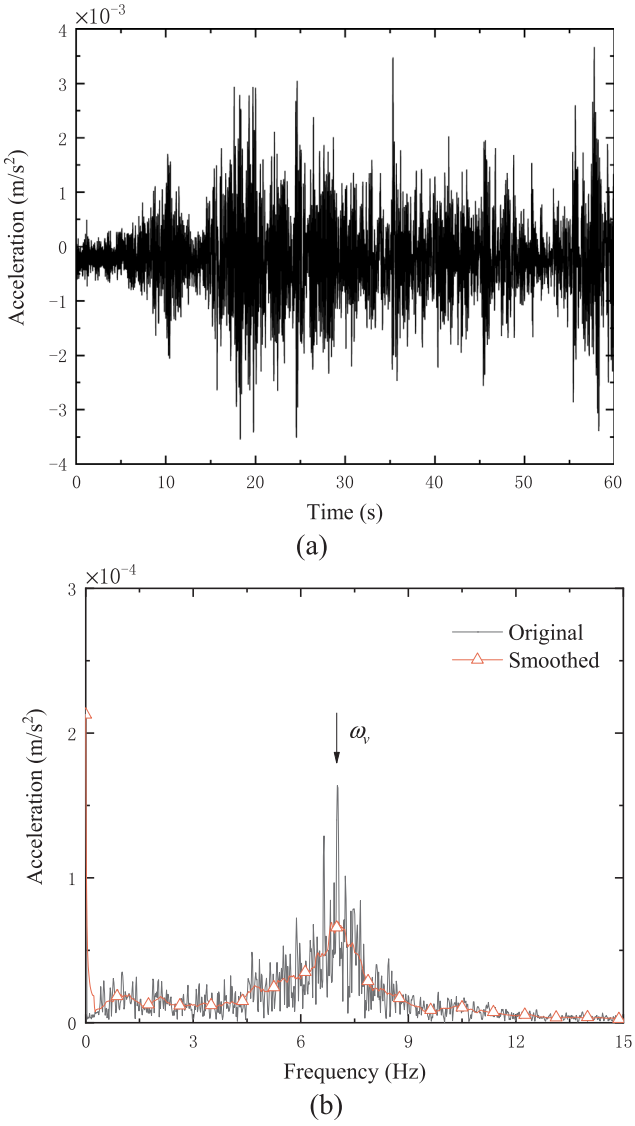

Fig. 17. Responses of the moving vehicle on flat road: (a) acceleration; (b) spectrum.

the non-moving state was verified to be good for both the car-body and contact-point responses. The purpose herein is to validate the applicability of the test vehicle to retrieving the bridge frequencies in the "moving state". The test bridge has a total length of only 55.2 m, which is generally short for a vehicle to pass at a certain speed. In testing the capability of the self-designed test vehicle, the first focus is on its transmissibility to receive the vibration information of the underlying bridge or ground in the moving state, but not on its moving speed. Besides, the test bridge is quite short, only 55.2 m long, and its two side approaches are not in a condition good for accelerating the test vehicle. With such physical restraints, the test vehicle is allowed to move very slowly, roughly 0.32 m/s, in either the flat road or bridge field tests, to ensure that sufficient data are taken during each run of measurement.

7.1. Flat road test for vehicle frequency in the moving state

To have the vehicle frequency identified is the first issue in application of the VSM, since it may overshadow the bridge frequencies and in many cases has to be eliminated or filtered out first. In the non-moving state, the vehicle frequency has been identified to be 9.09 Hz. Since the test vehicle will be towed by the tractor in the moving state, it is suspected that certain disturbance may be brought to the car body through the linkage between the tractor and trailer, which may result in variation of the vehicle frequency. Structurally speaking, the test vehicle has only two supports (contact points) on the ground. To be self stable, it should have the linkage with the front tractor as the third support. However, if the centerline of the tractor is *not well aligned* with that of the test vehicle, *some rotating motion* about the axis normal to the ground will be excited, resulting in a *yawing frequency* (of smaller peak) in addition to the *vertical frequency* (of larger peak) commonly known for the test cart. This was the technical issue encountered in preparing the first version of the paper, which is not shown here.

With the centerline of the tractor well aligned with that of the test vehicle, a flat (ground) road test is conducted for the moving vehicle, for which the acceleration response and spectra of the moving vehicle were plotted in Fig. 17(a) and (b), respectively. From the acceleration spectra in Fig. 17(b), especially the smoothed one, a distinct peak can be identified for the (vertical) vehicle frequency, which is $\omega_v = 6.90$ Hz. The lesson herein is that the idea of designing the vehicle as a single DOF system can be materialized in the moving state, only when the tractor is perfectly aligned with the test vehicle along the direction of movement. This depends mainly on the design of a proper linkage between the tractor and test vehicle.

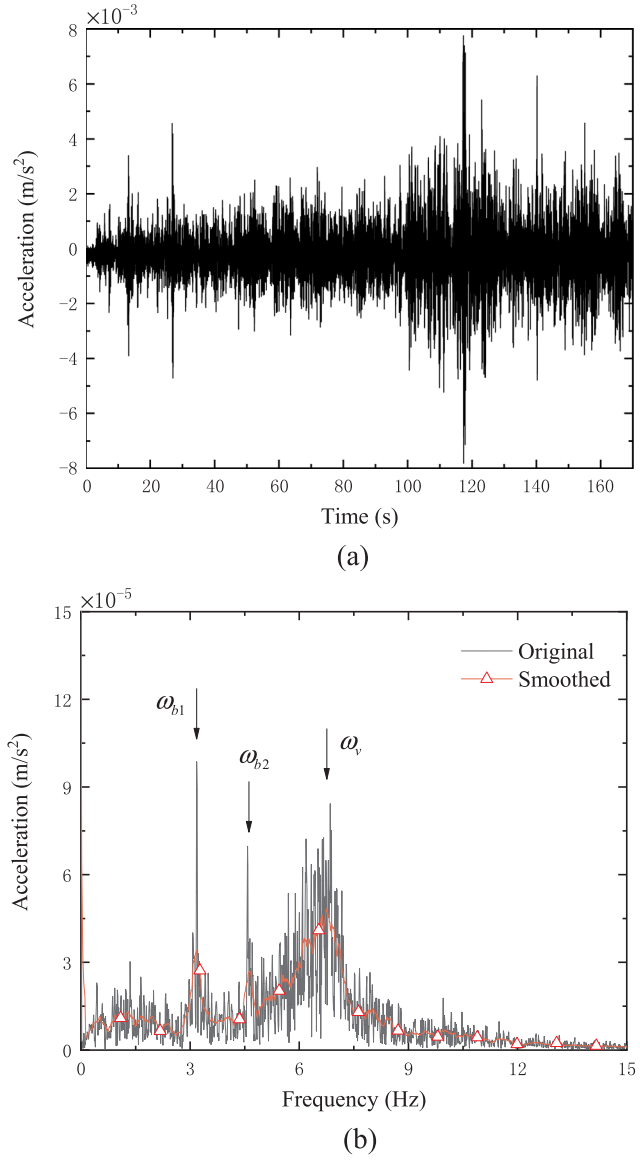

Fig. 18. Responses of test vehicle moving along centerline: (a) acceleration; (b) spectrum.

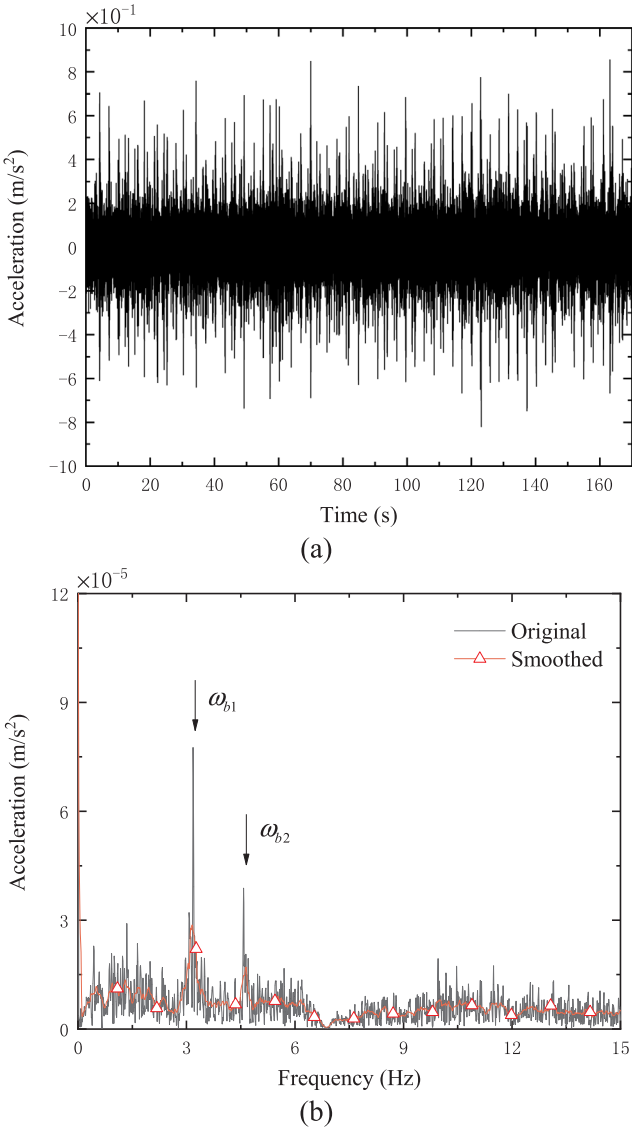

Fig. 19. Contact-point responses of test vehicle moving along centerline: (a) acceleration; (b) spectrum.

7.2. Case studies for extraction of bridge frequencies

In this section, two scenarios will be considered for the test vehicle for it to move over the bridge. In moving state, three runs of test were conducted for each scenario, and the results of all test runs are similar because of the same method adopted. It is confirmed that the results of this experiment are repeatable, as there is no ongoing traffic on the bridge. In the following, only the result of one test run will be presented for each scenario. Both the car-body and contact-point responses will be analyzed for extraction of the bridge frequencies. To excite the bridge to the level that can be measured, a group of people were employed to jump randomly and continuously on the bridge during the passage of the test vehicle. The data acquisition system is turned on when the test vehicle enters the bridge, and off when it leaves the bridge. The following are the two scenarios considered:

7.2.1. Scenario 1: vehicle moving along the bridge centerline

The time history acceleration recorded of the test vehicle was shown in Fig. 18(a), from which the effect of jumping on the bridge can be clearly observed. Correspondingly, the FFT spectra of the original data of the test vehicle have been plotted in Fig. 18(b) in black and the smoothed data by MAF in red. As can be seen, three peaks exist in Fig. 18(b). When compared with the previous measurements, the first two frequencies should be recognized as the bridge frequencies, and the third frequency as the vehicle frequency. Here one observes that once the vehicle is set in the moving state, many factors get involved, such as the linkage, road surface roughness, environment noise, and vehicle frequencies, etc., making it difficult to identify the bridge frequencies of the 3rd modes and higher.

It was found that the vehicle frequency ω_v appearing in the vehicle response of Fig. 18(b) has a high peak, which tends to hinder the visibility of bridge frequencies. To eliminate such an effect, one may calculate the contact-point response of the test vehicle using the backward substitution procedure given in Eq. (2). The acceleration response and FFT spectra of the contact point of the test vehicle have been plotted in Fig. 19(a) and (b), respectively. A comparison of Fig. 18(b) with Fig. 19(b) indicates that the vehicle frequencies have been filtered out and the bridge frequencies become clearly outstanding for identification.

7.2.2. Scenario 2: vehicle moving along the centerline with a temporary parking for 30 s

In this scenario, the test vehicle is allowed to move over the bridge,

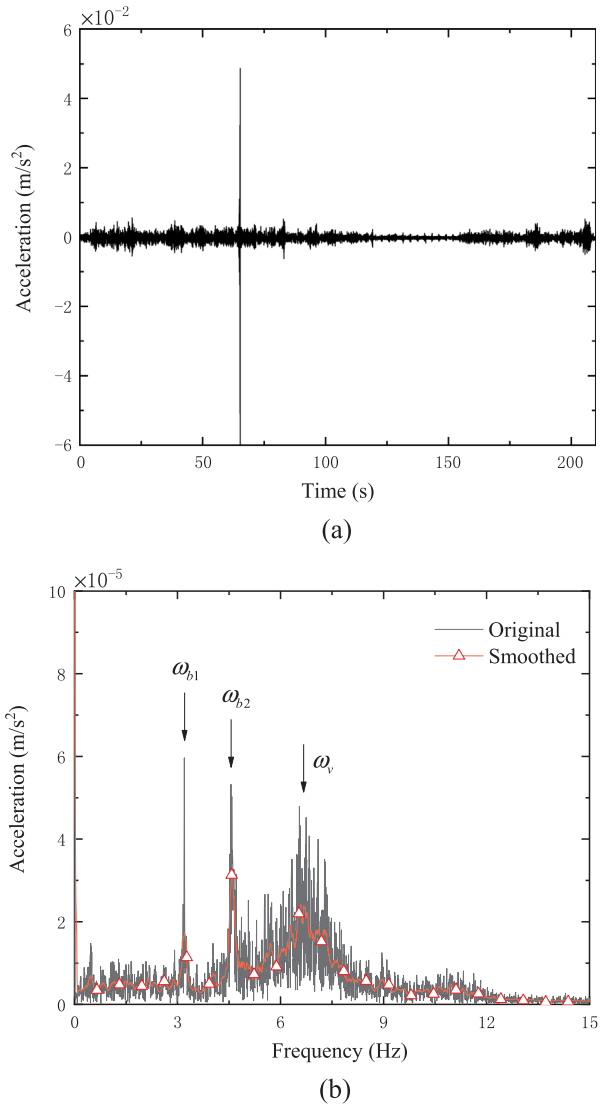

Fig. 20. Responses of test vehicle moving along the centerline with temporary parking: (a) acceleration; (b) spectrum.

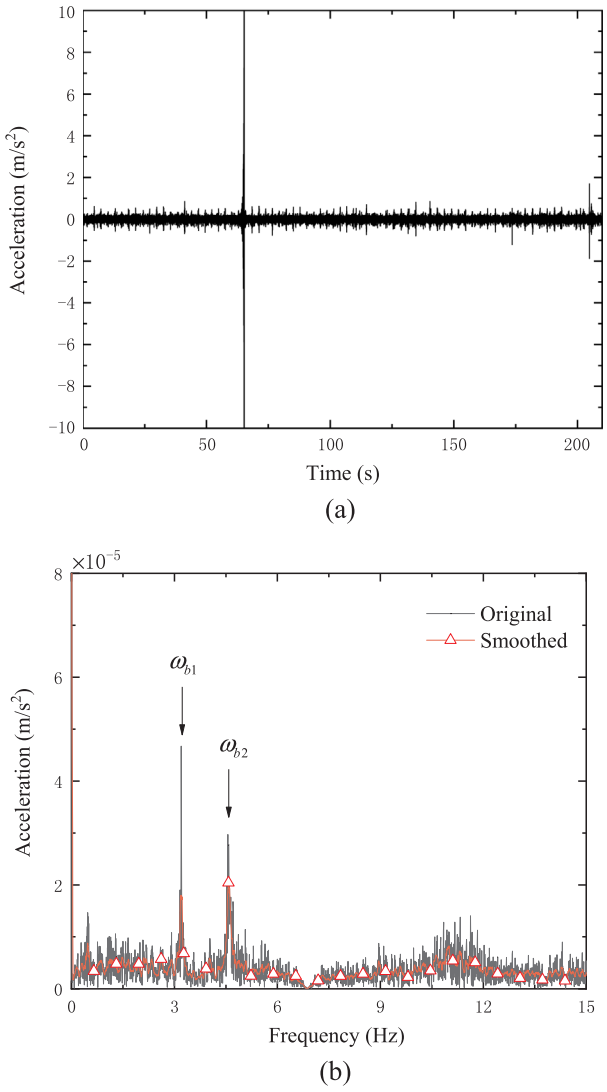

Fig. 21. Contact-point responses of test vehicle moving along centerline with temporary parking: (a) acceleration; (b) spectrum.

but with a temporary parking of 30 s in the middle of the first span of the bridge. As a matter of fact, we need not require a test vehicle to move in a non-stop manner over the bridge in the field test. Under certain circumstances, if a test vehicle is allowed to park for a while at some location of the bridge, it would help in collecting more sufficient data for the bridge in a single test.

The high peak in the time history of acceleration of the vehicle in Fig. 20(a) occurs at about 70 s is caused by the small impact when the vehicle stops moving. Correspondingly, the FFT spectra, including the original and smoothed ones, of the test vehicle response have been plotted in Fig. 20(b), from which three frequencies are identified to be the same as those in Fig. 18(b). Using the back-substitution procedure, the acceleration response and FFT spectra, including the original and smoothed ones, of the contact point of the test vehicle have been plotted in Fig. 21(a) and (b), respectively. From the result in Fig. 21(b), one observes that the first two bridge frequencies have been made more outstanding, the vehicle frequencies have been eliminated, and the noise level has been significantly reduced.

In the above two scenarios, it has been demonstrated that the first two bridge frequencies can be extracted successfully by the self-designed test vehicle in the moving state. The result obtained from the contact-point appears to be more outstanding than those from the car-body response. By switching the test vehicle from the non-moving to the moving state, the performance of the present devices deteriorates such that no frequencies of the 3rd mode and higher can be detected for the bridge. The first two bridge frequencies extracted from the test vehicle in the non-moving and moving states, along with those of the direct measurement, have been listed in Table 2. As can be seen, they all agree excellently.

8. Conclusions

In this paper, a self-made test vehicle is used to measure the frequencies of a bridge in both the non-moving and moving states. The self-made test vehicle fitted with vibration sensors is a two-wheel trailer, intentionally used to simulate the single-degree-of-freedom system that was theoretically adopted. The two-span bridge selected is located in the Chongqing University campus. Due to lack of structural

Table 2
The first two bridge frequencies extracted from VSM and direct method.

Methods	ω_{b1}(Hz)	ω_{b2}(Hz)
VSM	3.06	4.48
Direct method	3.08	4.49

data for the bridge, the results obtained by the test vehicle were compared with those obtained through attachment of vibration sensors on the bridge surface. By a backward procedure, the contact-point response of the vehicle with the bridge surface was calculated from the measured car-body response.

The following are the conclusions drawn in this study using the present devices and for the bridge tested:

(1) The transmissibility of the test vehicle in the non-moving state is good, in that all the frequencies detected by direct measurement can be caught by the test vehicle, including the torsional ones.
(2) The contact-point response calculated by the backward substitution procedure is verified to be free of the vehicle frequency, in consistence with the theoretical finding of the literature.
(3) For the test vehicle in the moving state, the bridge frequencies identified from the contact-point response appear to be more outstanding than those from the car-body response.
(4) The test vehicle in the non-moving state allows one to catch more bridge frequencies than in the moving state.
(5) Using the present devices and procedure, the first two frequencies can be retrieved of the bridge from the test vehicle either in the non-moving or moving states.
(6) The linkage between the tractor and trailer is an issue critical to the performance of the test vehicle in the moving state. It is required that the tractor be in perfect alignment with the test vehicle along the direction of movement, so as to avoid any possible yawing motion on the test vehicle.

Declaration of Competing Interest

The authors declare that they have no known competing financial interests or personal relationships that could have appeared to influence the work reported in this paper.

Acknowledgements

The senior author likes to thank The Fengtay Foundation for endowment of the Fengtay Chair Professorship. This research reported herein is sponsored by the following agencies: National Natural Science Foundation of China (Grant No. 51678091), Chongqing Municipal Natural Science Foundation (Grant No. cstc2017zdcy-yszxX0006), and Graduate Research and Innovation Foundation of Chongqing (Grant No. CYB18034).

References

[1] McLamore VR, Hart GC, Stubbs IR. Ambient vibration of two suspension bridges. J Struct Div-ASCE 1971;97(ST10):2567–83.
[2] Abdel-Ghaffar AM, Housner GW. Ambient vibration tests of suspension bridge. J Eng Mech Div-ASCE 1978;104(EM5):983–99.
[3] Adams RD, Cawley P, Pye CJ, Stone BJ. A vibration technique for non-destructively assessing the integrity of structures. Int J Mech Eng Sci 1978;20(2):93–100.
[4] Doebling SW, Farrar CR, Prime MB, Shevitz DW. Damage identification and health monitoring of structural and mechanical systems from changes in their vibration characteristics: a literature review. Los Alamos, NM: Los Alamos National Laboratory; 1996. Technical Report LA-13070-MS.
[5] Farrar CR, Doebling SW, Nix DA. Vibration-based structural damage identification. Philos Trans R Soc Lond Ser A-Math Phys Eng Sci 2001;359(1778):131–49.
[6] Huang CS, Yang YB, Lu LY, Chen CH. Dynamic testing and system identification of a multi-span highway bridge. Earthq Eng Struct Dyn 1999;28(8):857–78.
[7] Smyth AW, Pei JS, Masri SF. System identification of the Vincent Thomas suspension bridge using earthquake records. Earthq Eng Struct Dyn 2003;32(3):339–67.
[8] Ward HS. Traffic generated vibrations and bridge integrity. J Struct Eng-ASCE 1984;110(10):2487–98.
[9] Bu JQ, Law SS, Zhu XQ. Innovative bridge condition assessment from dynamic response of a passing vehicle. J Eng Mech-ASCE 2006;132(12):1372–9.
[10] Chen J, Xu YL, Zhang RC. Modal parameter identification of Tsing Ma suspension bridge under Typhoon Victor: EMD-HT method. J Wind Eng Ind Aerod 2004;92:805–27.
[11] Doebling SW, Farrar CR, Prime MB. A summary review of vibration-based damage identification methods. Shock Vib Digest 1998;30(2):91–105.
[12] Carden EP, Fanning P. Vibration based condition monitoring: a review. Struct Health Monit 2004;3(4):355–77.
[13] Fan W, Qiao PZ. Vibration-based damage identification methods: a review and comparative study. Struct Health Monit 2011;10(1):83–111.
[14] Yang YB, Lin CW, Yau JD. Extracting bridge frequencies from the dynamic response of a passing vehicle. J Sound Vib 2004;272:471–93.
[15] Yang YB, Yang JP, Zhang B, Wu YT. Vehicle Scanning Method for Bridges. London: John Wiley & Sons; 2019.
[16] González A, Obrien EJ, McGetrick PJ. Identification of damping in a bridge using a moving instrumented vehicle. J Sound Vib 2012;331(18):4115–31.
[17] Yang YB, Li YC, Chang KC. Constructing the mode shapes of a bridge from a passing vehicle: a theoretical study. Smart Struct Syst 2014;13(5):797–819.
[18] Malekjafarian A, OBrien EJ. Identification of bridge mode shapes using short time frequency domain decomposition of the responses measured in a passing vehicle. Eng Struct 2014;81:386–97.
[19] Zhang Y, Zhao HS, Lie ST. Estimation of mode shapes of beam-like structures by a moving lumped mass. Eng Struct 2019;180:654–68.
[20] Yang YB, Zhang B, Chen YN, Qian Y, Wu YT. Bridge damping identification by vehicle scanning method. Eng Struct 2019;183:637–45.
[21] Yang YB, Chang KC. Extracting the bridge frequencies indirectly from a passing vehicle: parametric study. Eng Struct 2009;31:2448–59.
[22] Yang YB, Chang KC. Extraction of bridge frequencies from the dynamic response of a passing vehicle enhanced by the EMD technique. J Sound Vib 2009;322:718–39.
[23] Yang YB, Li YC, Chang KC. Using two connected vehicles to measure the frequencies of bridges with rough surface: a theoretical study. Acta Mech 2012;223:1851–61.
[24] Yang YB, Chang KC, Li YC. Filtering techniques for extracting bridge frequencies from a test vehicle moving over the bridge. Eng Struct 2013;48:353–62.
[25] Yang YB, Zhang B, Qian Y, Wu YT. Contact-point response for modal identification of bridges by a moving test vehicle. Int J Struct Stab Dyn 2018;18(5):1850073.
[26] Yang YB, Zhang B, Wang TY, Xu H, Wu YT. Two-axle test vehicle for bridges Theory and applications. Int J Mech Sci 2019;152:51–62.
[27] Zhu XQ, Law SS. Wavelet-based crack identification of bridge beam from operational deflection time history. Int J Solids Struct 2006;43:2299–317.
[28] Khorram A, Bakhtiari-Nejad F, Rezaeian M. Comparison studies between two wavelet based crack detection methods of a beam subjected to a moving load. Int J Eng Sci 2012;51:204–15.
[29] Kim CW, Kawatani M. Pseudo-static approach for damage identification of bridges based on coupling vibration with a moving vehicle. J Struct Infrastruct Eng 2008;4(5):371–9.
[30] Zhang Y, Wang L, Xiang ZH. Damage detection by mode shape squares extracted from a passing vehicle. J Sound Vib 2012;331(2):291–307.
[31] Oshima Y, Yamamoto K, Sugiura K. Damage assessment of a bridge based on mode shapes estimated by responses of passing vehicles. Smart Struct Syst 2014;13(5):731–53.
[32] Obrien EJ, Malekjafarian A. A mode shape-based damage detection approach using laser measurement from a vehicle crossing a simply supported bridge. Struct Control Health Monit 2016;23:1273–86.
[33] Li ZH, Au FTK. Damage detection of bridges using response of vehicle considering road surface roughness. Int J Struct Stab Dyn 2015;15(3):1850073.
[34] Yau JD, Yang JP, Yang YB. A wavenumber-based technique for detecting slope discontinuity in simple beams using the moving test vehicle. Int J Struct Stab Dyn 2017;17(6):1750060.
[35] Zhang B, Qian Y, Wu YT, Yang YB. An effective means for damage detection of bridges using the contact-point response of a moving test vehicle. J Sound Vib 2018;419:158–72.
[36] Lin CW, Yang YB. Use of a passing vehicle to scan the fundamental bridge frequencies: an experimental verification. Eng Struct 2005;27:1865–78.
[37] Siringoringo DM, Fujino Y. Estimating bridge fundamental frequency from vibration response of instrumented passing vehicle: analytical and experimental study. Adv Struct Eng 2012;15(3):417–33.
[38] Yang YB, Chen WF, Yu HW, Chan CS. Experimental study of a hand-drawn cart for measuring the bridge frequencies. Eng Struct 2013;57:222–31.
[39] Chang KC, Kim CW, Kawatani M. Feasibility investigation for a bridge damage identification method through moving vehicle laboratory experiment. Struct Infrastruct Eng 2014;10(3):328–45.
[40] Malekjafarian A, McGetrick PJ, Obrien EJ. A review of indirect bridge monitoring using passing vehicles. Shock Vib 2015;2015:286139.
[41] Yang YB, Yang JP. State-of-the-art review on modal identification and damage detection of bridges by moving test vehicles. Int J Struct Stab Dyn 2018;18(2):1850025.
[42] Lyons RG. Understanding Digital Signal Processing. 3rd ed. Boston: Prentice-Hall; 2011.